Conservation in the CYP51 Family. Role of the B′ Helix/BC Loop and Helices F and G in Enzymatic Function†

Galina I. Lepesheva,*,‡ Cornelia Virus,§ and Michael R. Waterman

Department of Biochemistry, Vanderbilt University School of Medicine, Nashville, Tennessee 37232-0146

Received April 28, 2003; Revised Manuscript Received June 9, 2003

ABSTRACT: CYP51 (sterol 14α-demethylase) is an essential enzyme in sterol biosynthetic pathways and the only P450 gene family having catalytically identical orthologues in different biological kingdoms. The proteins have low sequence similarity across phyla, and the whole family contains about 40 completely conserved amino acid residues. Fifteen of these residues lie in the secondary structural elements predicted to form potential substrate recognition sites within the P450 structural fold. The role of 10 of these residues, in the B′ helix/BC loop, helices F and G, has been studied by site-directed mutagenesis using as a template the soluble sterol 14α-demethylase of known structure, CYP51 from *Mycobacterium tuberculosis* (MT) and the human orthologue. Single amino acid substitutions of seven residues (Y76, F83, G84, D90, L172, G175, and R194) result in loss of the ability of the mutant MTCYP51 to metabolize lanosterol. Residual activity of D195A is very low, V87A is not expressed as a P450, and A197G has almost 1 order of magnitude increased activity. After purification, all of the mutants show normal spectral properties, heme incorporation, and the ability to be reduced enzymatically and to interact with azole inhibitors. Profound influence on the catalytic activity correlates well with the spectral response to substrate binding, effect of substrate stabilization on the reduced state of the P450, and substrate-enhanced efficiency of enzymatic reduction. Mutagenesis of corresponding residues in human CYP51 implies that the conserved amino acids might be essential for the evolutionary conservation of sterol 14α-demethylation from bacteria to mammals.

CYP51[1] (sterol 14α-demethylase, 14αDM) is the only family in the cytochrome P450 superfamily which serves the same function in different biological kingdoms (*1*, *2*). It catalyzes oxidative removal of the 14α-methyl group from four naturally occurring Δ8-sterols (*3*−*5*). The reaction includes three steps of successive conversion of the 14α-methyl group to 14α-hydroxymethyl, 14α-carboaldehyde, and 14α-formyl intermediates followed by elimination of formic acid with concomitant introduction of the Δ14,15 double bond into the sterol core (*4*). The substrates of 14αDM differ only in the composition of the side chain [lanosterol (LS), 24,25-dihydrolanosterol (DHL), 24-methylene-DHL] or absence of one methyl group at the C4 in the sterol core (obtusifoliol) (Supporting Information). As a result of their structural similarity, the natural substrates are often easily interchangeable in the reconstituted reactions in vitro (*6*−*8*), and there are no other known substrates or reactions catalyzed by a CYP51. It has been suggested that 14αDM is evolutionarily the oldest P450, which arose in the prokaryotic era and spread into the other kingdoms with essentially the same catalytic role (*9*, *10*). Sterol biosynthetic pathways are well established in mammals, plants, and fungi (cholesterol, phytosterols, and ergosterol, respectively) (*2*). Inhibition of 14αDM is lethal in yeast, where it is the primary target of azole drugs widely used for treatment of fungal infections (*11*, *12*). It is not yet clear whether it is essential in bacteria; however, in addition to CYP51 from *Mycobacterium tuberculosis* (MT), whose structure in complex with azole inhibitors has been solved (*13*), 14αDM has been found in *Methylococcus capsulatus* (*14*) and *Mycobacterium smegmatis* (*15*), and a probable CYP51 gene is present in *Mycobacterium avium* (http://www.tigr.org).

Being evolutionarily distant, CYP51 family members have low sequence identity across phyla (22−32%), the whole family containing only about 40 completely conserved residues (less than 10% of an average P450 sequence). Fifteen of these residues lie in the secondary structural elements of MTCYP51, predicted to function as potential substrate recognition sites (SRSs) of a molecule having the P450 fold. The original prediction of P450 SRSs (*16*) was made for the largest and most catalytically diverse CYP family (CYP2) on the basis of the finding that the substrate-contacting regions in the crystal structure of CYP101 align with the six CYP2 sequences of highest amino acid variability where substitution of a single residue can strongly affect catalytic preferences or completely alter substrate specificity (*17*−*19*). The location of substrate binding residues in the same secondary structural elements has been

† This work was supported by NIH Grants GM37942 and ES00267-32 to M.R.W.

* To whom the correspondence should be addressed. Tel: 615-322-3318. Fax: 615-322-4349. E-mail: Galina.I.Lepesheva@vanderbilt.edu.

‡ Permanent address: Institute of Bioorganic Chemistry, National Academy of Sciences of Belarus, Minsk 220141, Belarus.

§ Current address: Department of Biochemistry, Saarland University, Saarbrücken, Germany.

[1] Abbreviations: CYP, cytochrome P450; CYP51 or 14αDM, sterol 14α-demethylase cytochrome P450; SRS, substrate recognition site; LS, lanosterol; DHL, dihydrolanosterol; MTCYP51, sterol 14α-demethylase from *Mycobacterium tuberculosis*; HPCD, 2-hydroxypropyl-*β*-cyclodextrin; WT, wild type; Fld, flavodoxin; Fdr, flavodoxin reductase; HPLC, high-performance liquid chromatography.

10.1021/bi034663f CCC: $25.00
Published on Web 07/11/2003

found in other CYPs, both by crystallography (*20*−*22*) and by site-directed mutagenesis (*23*−*29*).

In this study we have chosen for site-directed mutagenesis the 10 conserved residues from the three N-terminal SRSs, B′ helix/BC loop (SRS1), C-terminal part of the F helix (SRS2), and N-terminal part of helix G (SRS3). We have explored effects of substitution of the conserved residues on CYP51 function to test the notion that high conservation of the amino acid composition in these regions represents an important structural basis for evolutionary conservation of sterol 14α-demethylation. The results show a profound effect of the substitutions on the catalytic activity of sterol 14αDM directly connected with formation of the functional enzyme/substrate complex.

EXPERIMENTAL PROCEDURES

[3-^{3}H]Lanosterol (LS) was from American Radiolabeled Chemicals, Inc. (St. Louis, MO), Triton X-100 from Roche (Indianapolis, IN), and 2-hydroxypropyl-β-cyclodextrin (HPCD) from Sigma (St. Louis, MO). The other chemicals were purchased as previously indicated (*30*). Recombinant *Escherichia coli* flavodoxin (Fld) and flavodoxin reductase (Fdr) were expressed and purified as described (*31*). The absolute and difference reduced carbon monoxide complex (CO) and type I and type II binding spectra were all monitored using a DU 640 spectrophotometer (Beckman).

Site-Directed Mutagenesis. The strategy for mutagenesis was based on the alignment of MTCYP51 and sequences of other CYP51 family proteins from bacteria, plants, animals, and fungi. Mainly, we used alanine screening for the amino acid substitution. The choice of other residues was based on their particular properties: polarity, side chain length, or propensity to participate in formation of secondary structural elements. Site-directed mutagenesis was carried out using the QuikChange site-directed mutagenesis kit (Stratagene) and confirmed by DNA sequencing. As a template for mutagenesis of MTCYP51 we used its cDNA cloned in the pET17b expression vector (Novagen) (*6*). For mutagenesis of human CYP51 part of its cDNA was removed from the pCW expression vector (*32*) by *Nde*I/*Hin*dIII restriction and ligated into the same sites in pET17b. After mutagenesis *Nco*I/*Hin*dIII fragments of mutated human CYP51 were recloned into pCW and sequenced again to ensure proper ligation.

CYP51 Expression and Purification. MTCYP51 was expressed and purified as described previously (*30*). In the case of human CYP51 expression, the temperature was 26 °C (48 h after induction); Triton X-100 was added to final concentration 0.4% to the resuspended cells before sonication. P450 concentration was calculated from CO spectra (*33*). To estimate enzymatic activity of the MTCYP51 mutants in sonicated cell lysates, the samples were concentrated up to 20 ± 5 μM using an ultrafiltration membrane Centriprep YM-50. The final concentration of P450 in the reaction was 2 μM. To purify human CYP51, the sonicated cell lysate was incubated for 1 h on ice, and cell debris was removed by ultracentrifugation for 30 min at 68000*g*. Supernatant was diluted with 50 mM Tris-HCl (pH 7.4), containing 20% glycerol, 0.1 mM PMSF, 0.4% Triton X-100, and 20 mM mercaptoethanol (buffer A), and applied onto the Ni^{2+}-nitriloacetic acid−agarose (Qiagen, Valencia, CA) column equilibrated with the same buffer. The column was washed with buffer A, then buffer A containing 500 mM sodium chloride, and finally 20 mM Tris-HCl (pH 7.4) containing 20% glycerol, 0.1 mM PMSF, and 0.1% Triton X-100 (buffer B). The protein was eluted with buffer B containing 80 mM imidazole, diluted 10 times with buffer B, and applied onto a hydroxyapatite Bio-Gel (Bio-Rad) column equilibrated with the same buffer. After being washed with equilibrating buffer CYP51 was eluted with a linear gradient of 10−250 mM phosphate buffer (pH 7.4), containing 0.1% Triton X-100 and 20% glycerol, concentrated up to ∼100 μM, dialyzed against buffer B, and stored at −70 °C.

Enzymatic Activity. 14αDM activity of wild type (WT) and mutant forms of MT and human CYP51 was determined as previously described (*30*, *32*) with certain modifications. Briefly, radiolabeled [3-^{3}H]LS (100000 cpm)/cold LS (25 nmol)/Tween 80 (0.5 mg) was used as a substrate mixture per one reaction. Before the reaction, concentrated proteins at the ratios P450:Fld:Fdr = 1:20:4 (M/M) for MTCYP51 and P450:P450 reductase:dilauroyl-α-phosphatidylcholine = 1:2:50 (M/M) for human CYP51 were incubated for 10 min at room temperature. The final sample volume was 500 μL and contained 2 μM P450 (1 μM for human CYP51), 20 mM MOPS (pH 7.4), 50 mM KCl, 5 mM $MgCl_2$, 10% glycerol (buffer C), 0.4 mg/mL isocitrate dehydrogenase, and 25 mM sodium isocitrate. The reaction was initiated by addition of NADPH, final concentration 5 mM. Sterols were extracted with ethyl acetate and analyzed by HPLC. Duplicate determinations of four separate experiments were performed.

Interaction with 14α-Methylsterols and Ketoconazole. Ligand-induced spectral changes were monitored in buffer C at P450 concentrations 1 and 5 μM (5 μM concentration was used to confirm the absence of spectral response in several mutants) at 24 °C. Highly hydrophobic LS or DHL was added from a 1 mM stock solution in 45% HPCD to diminish their precipitation in aqueous solutions (*34*). Ketoconazole was dissolved in DMSO at a stock concentration of 2 mM. For each mutant, three binding assays of eight ligand concentrations in the range of 0.5−20 μM for sterols and 0.5−60 μM for ketoconazole were performed. The concentrations of free ligand were calculated using the equation (*35*):

$$[L]_{free} = [L]_{total} - [P450]\Delta A/\Delta A_{max}$$

where $\Delta A_{390-420}$ and $\Delta A_{432-413}$ were taken from type I and type II binding spectra, respectively. Apparent dissociation constants and maximal spectral response per nanomole of P450 were determined by plotting absorbance changes calculated from each difference spectrum against the concentration of free ligand and fitting the data to a rectangular hyperbola using Sigma Plot Statistics. The spin state of P450 samples was estimated from the ratio ($\Delta A_{393-470}/\Delta A_{417-470}$) before and after interaction with substrate.

Efficiency of Enzymatic Reduction. Enzymatic reduction of MTCYP51 mutants was carried out at the conditions, protein ratio, and concentrations described for the activity measurements. The final volume was adjusted to 750 μL with water. Measurements were made without substrate or in the presence of 10 μM DHL. A 250 μL aliquotwas taken for the measurement of the CO spectrum of chemically reduced P450. Enzymatic reduction was started with the

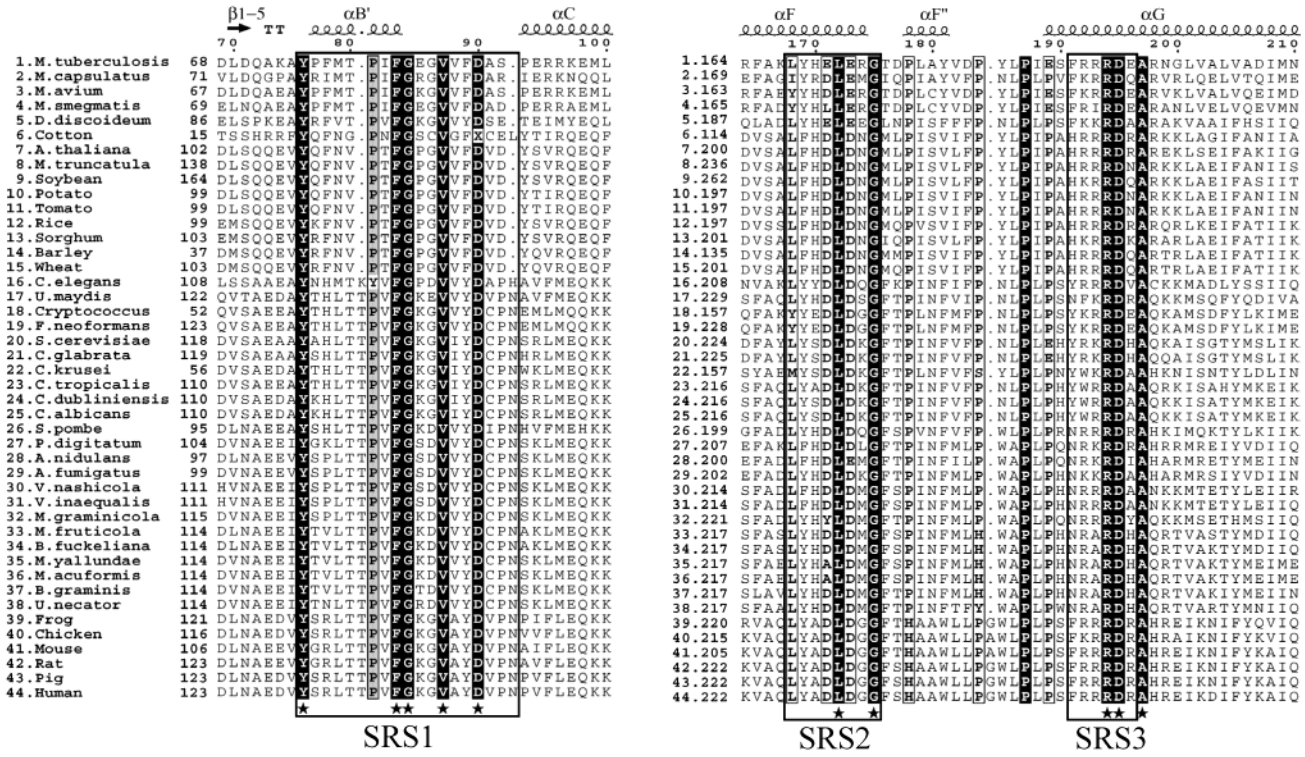

FIGURE 1: Sequence alignment of 44 CYP51 family members from different biological kingdoms [bacteria (*1*−*4*), mycetozoa (*5*), plants (*6*−*15*), fungi (*16*−*38*), and animals (*39*−*44*)] in the regions of the B′ helix/BC loop and helices F and G. The sequences were taken from NCBA, SWISS-PROT, TrEMBL, and TIGR databases. The alignment was performed using Clustal W1.81 and prepared in ESPript 2.0 programs. 100% and more than 95% conserved residues are shaded in black and gray, respectively. More than 85% conserved residues are taken in frames. Assignment of secondary structure elements is based on the MTCYP51 structure (PDB entry 1E9X). Predicted substrate recognition sites 1, 2, and 3 (*10*) are framed. Amino acid residues mutated in this study are marked with stars below the alignment. Full-length sequence alignment of the CYP51 family can be found in Supporting Information.

addition of NADPH. The solution was divided into two parts and CO gas was bubbled through the sample cuvette. Efficiency of enzymatic reduction was calculated as the maximal amount of P450−CO complex formed during the time course measurement taken as a percentage of P450 detected in the chemically reduced aliquot: $\Delta A_{450-490}$(NADPH)/$\Delta A_{450-490}$($Na_2S_2O_4$) (%).

Heme Pocket Stability. The percentage of P450 recovery in the reaction mixtures was calculated from the CO spectra taken at the beginning and at the end of the incubation time (20 min). Samples were incubated at 37 °C in the presence of substrate and NADPH, in the absence of substrate, and in the absence of substrate and NADPH. Stabilities of the Na_2S_2O-reduced CO complexes of the mutants (2 μM) were compared as the half-times of P450 to P420 conversion ($\tau_{1/2}$) from time course measurements in buffer C in the presence and absence of substrate (DHL and LS, final concentration 10 μM).

RESULTS AND DISCUSSION

Correct assignment of secondary structural elements upon alignment or modeling is a major limitation in the designation of putative P450 SRSs. The problems are connected predominantly with SRS2 and SRS 3 because, in addition to the highest variability in the amino acid sequence in the CYPs having different substrate specificity, helices F, G, and the intervening loop vary considerably in length (*19*, *20*, *36*, *37*). As a result, the question about their participation in substrate binding in many mammalian P450s remains unclear. Solution of the MTCYP51 crystal structure showed the exact location of secondary structural elements in the protein sequence and allowed their assignment to other family members with high probability. The 10 conserved amino acids throughout the whole CYP51 family in the B′ helix/BC loop and helices F and G are seen in the alignment in Figure 1.

In the structure of MTCYP51 in complex with an azole inhibitor (Figure 2A) the BC loop forms a portion of the mouth of the substrate access channel, leading from the opening above the heme along the heme plane into the large, 2600 Å^3 cavity located on the distal side of the heme between the α- and β-domains (*13*). The B′ helix builds the top (ceiling) and contacts the C-terminal portion of helix F and N-terminal portion of helix G, which form part of the distal wall of this cavity. Panels B and C of Figure 2 show orientation of the side chains of the mutated residues in the access channel and substrate binding cavity relative to the heme and azole inhibitor.

Primary Screening of the MTCYP51 Mutants. Table 1 comprises a summary of structural information about the mutated residues and experimental results including expression of the mutants in the cytosolic fraction of *E. coli* cells in the P450 form and their ability to metabolize LS, presented in comparison to the WT. At this stage the activity measurements were carried out in the concentrated soluble fraction of *E. coli* cells after 2 h of enzymatic reaction to achieve maximal LS conversion.

In the region of SRS1 (B′ helix/BC loop), V87A is not expressed in the P450 form while the expression level and activity of the V87I mutant are comparable to WT. Substitu-

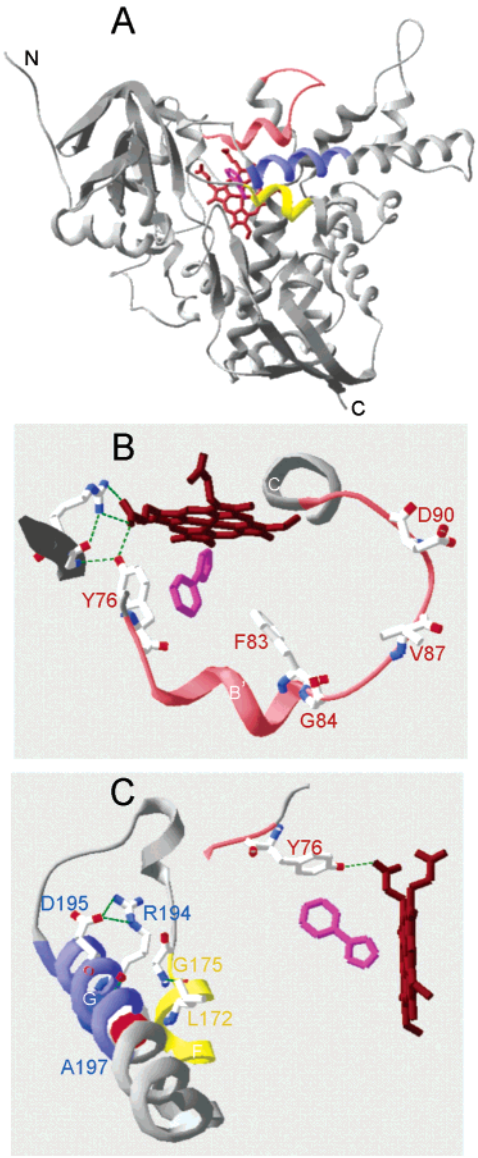

FIGURE 2: Location of the mutated conserved residues in the structure of MTCYP51 in complex with an azole. (A) Overall structure from distal view. (B) B′ helix/BC loop. (C) Helices F and G with orientation of the side chains of the mutated residues shown. The figures were generated in Swiss-PDB Viewer. Helices are shown as light gray and β-strands as thick dark gray arrows. Regions of mutagenesis are colored in red, yellow, and blue for the B′ helix/BC loop (SRS1), C-terminal part of helix F (SRS2), and N-terminal part of helix G (SRS3), respectively. Heme is presented in magenta and ligated 4-phenylimidazole in purple. A197 is shown as van der Waals surfaces. Hydrogen bonds mentioned in the text are presented in green.

tion of the other conserved residues (Y76, F83, G84, and D90) results in P450s with no detectable ability to metabolize LS. Y76 is one of the residues closest to the heme from the distal side, and its side chain OH group forms hydrogen bonds with the A-ring propionate and the main chain oxygen of M325 (β1−4, SRS5). Absence of any detectable activity in all of the Y76 mutants indicates that it is the properly positioned OH group and not the aromatic ring, which is essential functionally. The 2-fold decrease in P450 expression of Y76F with practically no change with further side chain modifications suggests that the OH group interactions are also favorable for heme incorporation but not crucial, probably because the propionate is also supported by a salt bridge with conserved R326. F83 lies closest to the heme in the ceiling of the substrate binding cavity (B′ helix) above the heme plane. Loss of activity after insertion of an OH group into the aromatic ring (F83Y) or substitution of the ring by alanine shows that both hydrophobicity and the shape (at least the length) of the side chain of this residue are important. G84 disrupts the B′ helix and begins the BC loop, which forms a large surface opening to the substrate access channel [a unique feature in the MTCYP51 P450 fold (*13*)]. D90 lies in the portion of the channel most open to the surface. Because of high flexibility of the region, its side chain in the structure is missing. Its negative charge is not important structurally as mutation D90A even slightly increases expression of enzymatically inactive P450.

While all of the mutated residues in SRS1 are visible through the opening in the MTCYP51 structure, the conserved amino acids in the helices F and G are shielded from the surface and are expected to participate in stabilization of the well-packed protein core. L172 (helix F) forms multiple van der Waals contacts with other hydrophobic residues (Table 1), including the side chain of R194 (helix G). The guanidinium group of R194 is neutralized by a salt bridge with the carboxylate of D195 and lies spatially close to P144 (helix E) and P81 (B′ helix). Oriented toward the heme, the side chain of L172 and the hydrophobic arm of R194 are seen from inside the substrate binding cavity. P450s that are quite well expressed but with no detectable activity are formed upon substitution of G175 [which similarly to G84 in SRS1 stops an α-helix (F) and starts a loop] and upon disruption of the salt bridge R194−D195 by substitution of R194A or D195A. Mutation of the arginine to another charged residue instead of R (R194K) in addition to enzyme inactivation results in a 5-fold decrease in P450 expression. The most profound negative effect of mutagenesis on P450 expression in this region is caused by decrease of hydrophobicity and size of the side chain in place of L172. In contrast to mutagenesis of V87, however, where mutants that are expressed are enzymaticaly active, well-expressed L172V shows only a trace of WT activity. L172G and L172A (3% and 11% of P450 expression, respectively) do not metabolize LS. The data suggest that while conservation of the long hydrophobic residue at position 87 is probably essential for folding, L172 in addition to its structural importance could play a specific functional role.

The last conserved residue in the putative SRS3 sequence, A197, is located in the middle of the G helix with the side chain oriented inside the protein globule and not accessible to the surface. Surprisingly, its replacement to glycine, a polar residue with low propensity to form helical structures, produces the mutant with enhanced enzymatic activity. Substitution of the A in this position with another polar residue (A197S) has practically no effect while the long hydrophobic chain of Leu decreases both expression and activity. To better understand the reasons for the observed functional changes, selected mutants were chosen for purification and further characterization.

Characterization of the Purified Proteins. (A) Basic Properties. No rapid decomposition or alteration in the heme content was observed upon purification. All of the mutants were purified from the soluble fraction of *E. coli* cells with essentially the same yield (about 40% after two successive chromatographic stages without detergent at more than 95%

Table 1: Structural and Functional Information on Mutated Conserved Amino Acid Residues of MTCYP51[a]

		structural data				experimental results[b]	
SRS	mutated residue	distance to iron, Å	side chain interactions	surface accessibility,[f] %	substitution	P450 expression, %[c]	LS 14α-demethylation, %[d]
1	Y76	9.6	h[g] (A ring propionate), M325	7	F	62 ± 7	nd[e]
					T	55 ± 9	nd
					A	51 ± 8	nd
	F83	11.1		25	Y	109 ± 12	nd
					A	94 ± 10	nd
	G84	18.3		12	A	73 ± 10	nd
					T	79 ± 11	nd
	V87	22.5		28	A	0	
					I	110 ± 5	104
	D90[j]	22.6		55	A	165 ± 12	nd
2	L172	16.8	w[h] (L82, Y169, R194, L211)	<1	G	3 ± 1	nd
					A	11 ± 3	nd
					V	72 ± 10	3 ± 0.5
	G175	18.3		<1	A	80 ± 7	nd
					T	76 ± 5	nd
3	R194	19.7	sb[i] (D195), w (P81, P184, L172)	1	A	53 ± 6	nd
					K	22 ± 7	nd
	D195	23.2	sb (R194)	22	A	68 ± 5	nd
	A197	22.6		1	G	108 ± 10	350 ± 22
					S	75 ± 9	65 ± 5
					L	25 ± 4	23 ± 3

[a] Expression levels of P450 were estimated from the reduced CO difference spectra; activity measurements were conducted as described in Experimental Procedures. [b] Data are expressed as the mean ± standard deviation of duplicate determinations of four independent experiments. [c] Expression of the WT is 150 ± 10 nmol/100 mL of *E. coli* culture. [d] Activity of the WT is 4.8 ± 0.6 nmol of lanosterol (nmol of P450)$^{-1}$ (2 h)$^{-1}$. [e] Not detected. [f] Percentage of the surface of the residue accessible to the solvent in MTCYP51 (1E9X) was calculated using the Swiss-PDB Viewer. [g] Hydrogen bonds. [h] van der Waals interactions. [i] Salt bridge. [j] The side chain of this residue is missing in the structure.

Table 2: Purification Yield and Spectral Characteristics[a] of MTCYP51 Mutants

			P450 stability		efficiency of reduction through Fld/Fdr, %
MTCYP51	yield,[b] %	A_{417}/A_{280}[c]	$\tau_{1/2}$ of denaturation in CO complexes (% of WT)[d]	recovery after enzymatic reaction, %	
WT	45	1.60	100 ± 11	68 ± 8	44 ± 5
Y76F	38	1.53	51 ± 6	40 ± 6	30 ± 4
F83Y	50	1.64	104 ± 9	75 ± 8	39 ± 6
G84A	41	1.56	55 ± 7	54 ± 8	25 ± 3
D90A	45	1.58	108 ± 8	78 ± 6	42 ± 4
L172A	35	1.50	22 ± 6	22 ± 5	43 ± 5
G175A	42	1.56	68 ± 8	63 ± 8	32 ± 4
R194A	40	1.60	27 ± 5	36 ± 3	37 ± 6
D195A	39	1.54	56 ± 7	61 ± 4	39 ± 4
A197G	40	1.65	67 ± 9	76 ± 4	43 ± 6

[a] Data from three experiments for each P450 mutant are presented as the mean ± standard deviation. [b] Percentage yield of detectable P450 in the *E. coli* soluble fraction after the two-step purification procedure. [c] Spectrophotometric index 1.6 corresponds to 18 nmol of heme/mg of protein. [d] $\tau_{1/2}$ of denaturation (half-time of conversion to P420) for the WT at the experimental conditions is 305 s.

electrophoretic purity), in the typical CYP51 low-spin state, a Soret peak at 417 nm, and OD_{417}/OD_{280} within 1.5−1.65 (Table 2). They remained in the P450 form upon storage at −70 °C, forming spectroscopically indistinguishable reduced CO complexes. However, CO complexes of several mutants showed an increase in the rate of conversion into the P420 form.

(B) Heme Pocket Stability. 14αDM from various species differ in stability of their reduced CO complexes (*38*), rapid P450 to P420 conversion being a specific feature of MTCYP51 (*39*). Half-times of denaturation sharply decrease for L172A and R194 mutants, destabilization also being observed for Y76F, G84A, G175A, D195A, and A197G, while rate of denaturation is similar to WT for F83Y and D90A (Table 2). To test whether the decrease in stability could be the reason for the absence of activity, we measured the amount of P450 recovered after the reconstituted enzyme reaction. Decrease in the detectable P450 peak without conversion into P420 is known to be connected with heme loss caused by hydrogen peroxide formation as a result of uncoupling of electron transport and substrate monooxygenation (*40*, *41*). For the WT MTCYP51 after 20 min incubation at 37 °C, heme loss is about 30%. Again, the greatest heme loss was observed for L172A and R194A, 78% and 64% of the original amount, respectively. Stabilities of the other mutants, with the exception of A197G (which was found even more stable than the WT), correlate well with the half-time of denaturation in the CO spectra (Table 2). In the control samples [without NADPH (data not shown)], however, all of the proteins reveal almost unchanged P450 level, implying that the destabilization of the heme pocket is local and primarily affects the reduced state of the enzyme.

(C) Efficiency of Enzymatic Reduction. To check directly whether the mutations influence the ability of the enzyme to accept electrons from NADPH through protein−protein interactions, we measured their efficiency of enzymatic

Table 3: Sterol 14αDM Activity and Ligand Binding of the Purified MTCYP51 Mutants[a]

		ligand binding			
		DHL (type I spectral response)		ketoconazole (type II spectral response)	
MTCYP51	14α-DM activity, min^{-1}	K_d, μM	ΔA_{max}/nmol (% high spin)	K_d, μM	ΔA_{max}/nmol
WT	0.14 ± 0.3 (0.26)[b]	1.30 ± 0.20	0.02 ± 0.005(18)	5.6 ± 0.8	0.08 ± 0.01
Y76F	nd	nd	nd	5.5 ± 1.36	0.09 ± 0.01
F83Y	nd	nd	nd	11.1 ± 0.7	0.05 ± 0.01
G84A	nd	nd	nd	5.7 ± 1.2	0.11 ± 0.02
D90A	nd	nd	nd	6.4 ± 0.83	0.07 ± 0.01
L172A	nd	nd	nd	7.1 ± 1.9	0.05 ± 0.01
G175A	nd	nd	nd	4.6 ± 0.8	0.09 ± 0.01
R194A	nd	nd	nd	3.3 ± 0.9	0.09 ± 0.01
D195A	nd (0.05)[b]	1.12 ± 0.24	0.007 ± 0.001 (6)	2.3 ± 0.4	0.09 ± 0.01
A197G	1.01 ± 0.16	1.91 ± 0.26	0.078 ± 0.004 (71)	3.9 ± 0.9	0.08 ± 0.01

[a] Parameters were determined as described in Experimental Procedures. [b] Activity detected at 5-fold increased (10 μM) final concentration of MTCYP51.

reduction. The endogenous electron donor for MTCYP51 is not known, it is not reduced by P450 reductase of the microsomal orthologues, and the *E. coli* Fld/Fdr reduction system is not highly efficient (*6*). The amount of P450, which can be reduced through Fld, was found to be about 40% of that detectable after chemical reduction with $Na_2S_2O_4$ (Table 2). Some decrease in the maximal amount of detectable P450 is demonstrated by Y76F and the two glycine mutants (1.5-, 1.8-, and 1.4-fold, respectively); all of the others are reduced with the efficiency similar to WT. Thus, the proteins basically preserve their ability to accept electrons through functional protein−protein interactions and are present in the P450 form after enzymatic reaction.

(D) Enzymatic Activity. Nevertheless, all of the mutants inactive in the *E. coli* soluble fraction also showed no LS conversion after purification (Table 3). Increase in the turnover number for A197G is by a factor of 7. The calculated rate of LS demethylation of the WT protein (0.14 min^{-1}) is within the range of values measured previously toward DHL (*30*) or obtusifoliol (*42*). Taking into consideration the low efficiency of enzymatic reduction of MTCYP51 and destabilization of the reduced state observed for several mutants in an attempt to detect residual activity, we varied the experimental conditions for the mutants with no detectable LS demethylation. Increased LS concentrations reduced the turnover number for the wild-type protein and did not give any product in the case of the mutants (data not shown). Increase of the amount of the enzyme used in the reconstitution assay by 5-fold at constant LS concentration and ratio P450:Fld:FdR (1:20:4, M/M) allowed us to achieve 86% of LS conversion per 20 min for the wild-type protein. But even at this concentration (10 μM) only one of the MTCYP51 mutants with no detectable activity at other conditions, D195A (salt bridge with R194), showed 20% of the wild-type protein LS 14α-demethylation (Table 3). Very small peaks with retention times corresponding to CYP51 intermediates (*30*, *43*) and no product formation were observed for D90A and L172A (Supporting Information).

(E) Ligand Binding. Interaction of P450 with substrates and azole inhibitors produces two different types of spectral changes. The type I spectral response (blue shift of the Soret band from 417 to 394 nm) upon substrate binding is caused by expulsion of the water molecule from the sixth coordination sphere of the heme iron, leading to its spin state change from hexacoordinated low to pentacoordinated high (*44*). Substrate does not form contacts with the iron, leaving a space of about 5 Å available for molecular oxygen to be activated (*45*). The type II spectral response results from direct coordination of a basic nitrogen of azole compounds with the low-spin heme iron. This complex formation is accompanied by a red shift in the Soret band (from 417 to 425−435 nm). In CYP51, probing the interaction with azole inhibitors is of practical importance because sterol 14αDM is the primary target for medicinal antifungal agents as well as an origin of azole resistance in certain pathogenic fungal strains as a result of CYP51 mutagenesis (*11*, *12*, *46*).

Inhibitory potency of azoles toward P450s strongly depends on the composition of their lipophilic portion which forms hydrophobic contacts within the P450 substrate binding cavity (*47*). Titration of the mutants with ketoconazole [having the highest affinity to MTCYP51 among tested azole inhibitors (*6*)], however, showed that none of the mutated residues is essential for the interaction with the ligand. Both the calculated apparent K_d and amplitude of the spectral changes differ little (Table 3), with the lowest affinity (2-fold increased K_d and 1.5-fold decrease in ΔA_{max}) being observed for F83Y and slightly changed shape of a spectrum (a plateau between 390 and 413 nm) produced by the D90A mutant (Figure 3).

On the contrary, titration of the inactive mutants (Y76, F83, G84, G175, L172, and R194) with substrates (LS/DHL) did not lead to any spectral response. First, the results point out that the detected loss of activity is definitely connected with the altered substrate binding properties of the mutants. Second, finding that the residues essential for formation of the enzyme/substrate complex are not required for the interaction with azole inhibitors indirectly explains the appearance of azole resistance in catalytically normal fungal CYP51. The data are in a good agreement with the structure of MTCYP51 with another inhibitor, fluconazole (1EA1), where the conserved residues studied also do not form any contacts with inhibitor (*13*).

Type I spectral responses of the remaining mutants are also profoundly different from the WT. D90A reveals spin state changes slowly appearing over time with a maximal amplitude of 35% of WT observed after 30 min. It may indicate that even in the absence of the aspartate the substrate molecule can finally reach the active center but cannot be demethylated. The data suggest that being a surface substrate recognition residue (*48*) D90 is also very likely to participate

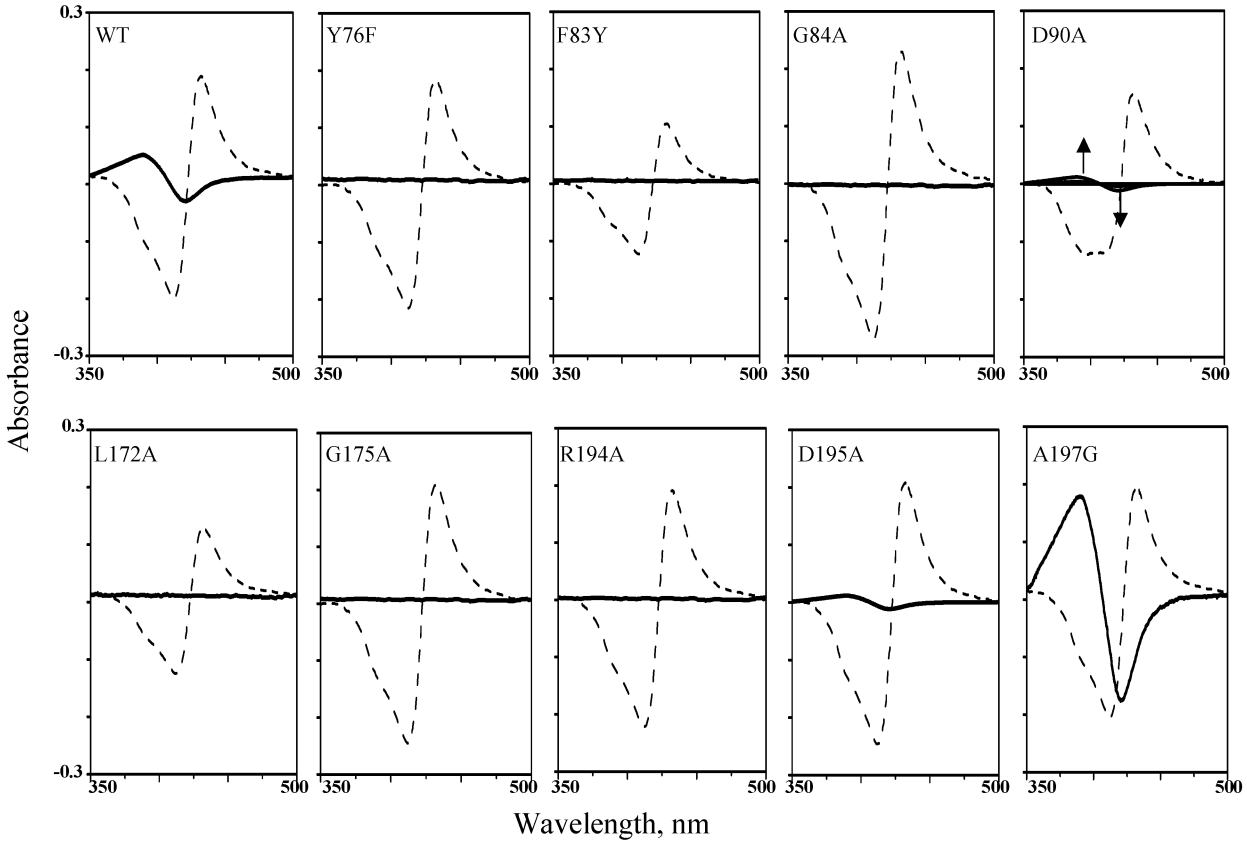

FIGURE 3: Spectral changes upon ligand binding to MTCYP51, WT, and mutants. Difference spectra were recorded with 5 μM P450 in buffer C. Final concentrations of DHL (solid line) and ketoconazole (dashed line) were 20 and 80 μM, respectively. The baseline spectra obtained in the presence of the same volumes of solvents (45% HPCD and DMSO) were subtracted. Type I spectral response of D90A is delayed in time; the arrows show directions of changes detected after 10 and 30 min.

in substrate orientation during catalysis. The suggestion is in good agreement with the detected ability of the mutant to produce a trace amount of intermediate at high protein concentration.

The amplitude of spin state changes of D195A and A197G correlates well with their activity (Table 3). Together with the unchanged affinity (apparent K_d), it points out that neither of these residues participates in substrate binding directly but their substitutions affect orientation or the amount of the bound substrate. Because of low solubility of the sterols the fraction of the P450 molecules, which change spin state upon titration with the substrates in vitro in the CYP51 family usually, does not exceed 10% (*42*, *43*, *49*). Using HPCD to dissolve the sterols allowed us to reach 18% spin state transition for WT. Spin state transition in the A197G upon titration with DHL reaches about 70% (Figure 4A). With LS it is slightly lower (55−60%). The difference between the two substrates is not seen for WT and may be due to either to slightly lower solubility of LS or some preference of the mutant toward the DHL side chain.

(F) Effect of Substrate on Mutant Stability and Enzymatic Reduction. It is known that substrate binding not only causes iron spin state transition but also increases redox potential as well as affinity of P450 interaction with electron donor proteins; many CYPs cannot be reduced enzymatically in the absence of substrate which in vivo prevents futile expenditure of reducing equivalents (*20*, *50*, *51*). The presence of substrate stabilizes P450 upon purification, storage, and enzymatic reaction (*41*, *52*). Here we found that substrate enhances the efficiency of enzymatic reduction and stabilizes MTCYP51 during the catalytic cycle and in the chemically reduced CO complexes. The effect is noticeable for the WT but significantly more pronounced for A197G (Figure 4B,C). In the presence of substrate its efficiency of enzymatic reduction as well as the percentage of detectable P450 after enzymatic reaction increases almost twice, and denaturation in the CO complexes occurs much slower. The differences in the expression of the effect correlate well with spin state transition upon substrate addition, suggesting that less than 20% of the WT protein molecules are in the complex with the substrate, while the fraction of substrate-bound A197G is 4-fold higher. Again, the inactive mutants are insensitive to the substrate addition and did not reveal any changes from the values presented in Table 2. Thus, even if the sterol molecule can reach the binding cavity of the mutated enzyme, participation of *all* of these conserved residues appears necessary for the substrate to be properly oriented and undergo the three steps of 14α-demethylation.

Mutagenesis of Human CYP51. Similar importance of amino acid conservation has been found upon mutagenesis of the membrane-bound human isoform of 14αDM. Here we mutated the five conserved residues in SRS1 which in MTCYP51 correspond to Y76, F83, G84, V87, and D90. In comparison with bacterial orthologues human CYP51 has much higher activity. In our reconstituted system the calculated LS turnover number is 16 min^{-1} (Table 4). The value is close to that published for rat CYP51 (14 min^{-1}) (*38*) and exceeds the rates detected for MT, *M. smegmatis* (*15*), and *M. capsulatus* CYP51 (*14*) 50−100-fold. It is likely that the slow rates of LS demethylation by bacterial 14αDM

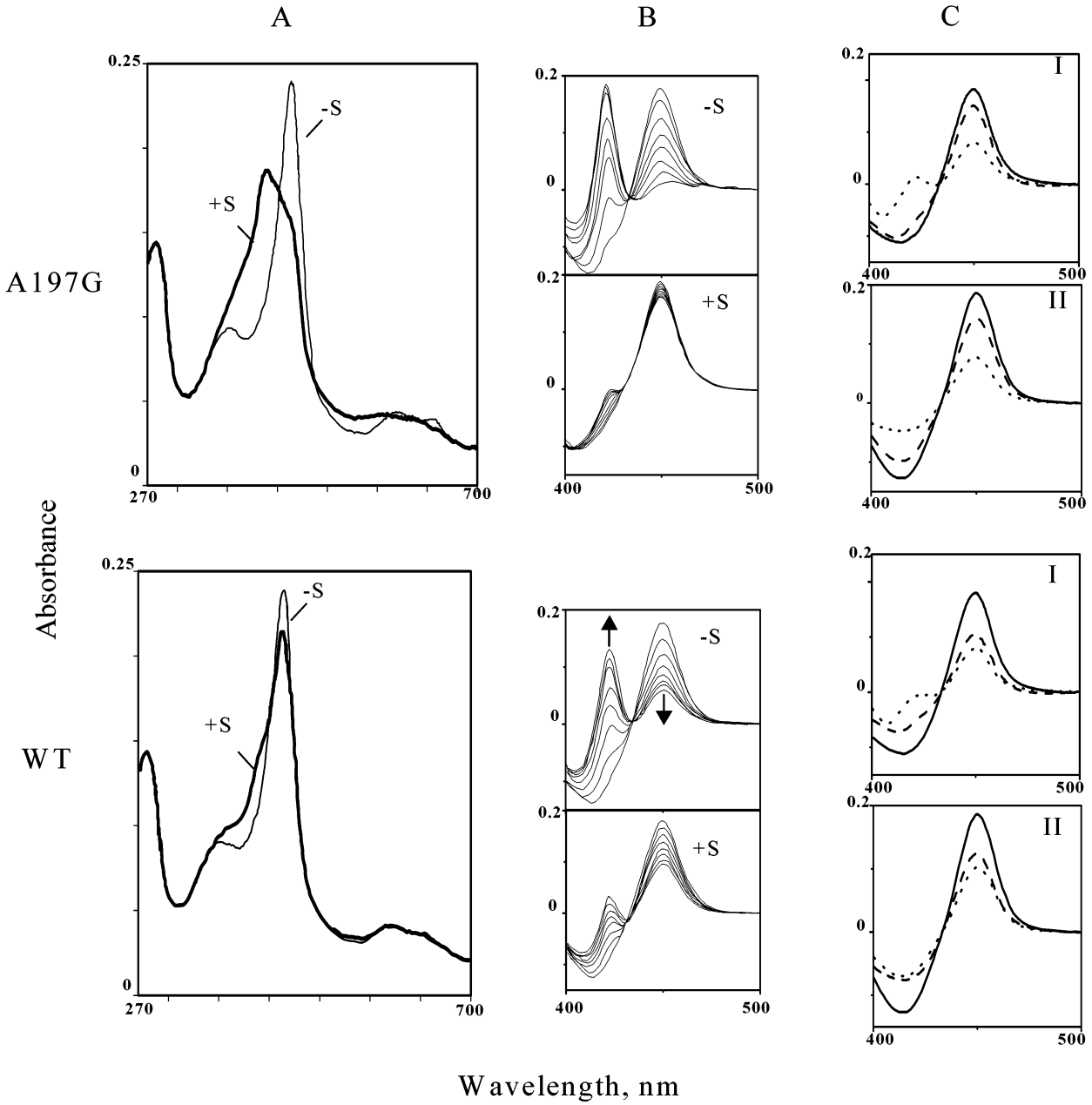

FIGURE 4: Effect of substrate on spectral properties of MTCYP51, WT, and A197G. (A) Absolute absorbance spectra before (−S) and after (+S) interaction with DHL at the enzyme/substrate ratio of 1:5 (M/M). (B) P450 to P420 conversion in the $Na_2S_2O_4$-reduced CO complexes. The time interval between the measurements was 1 min. Arrows show directions of changes. (C) (I) Efficiency of reduction with NADPH through the *E. coli* Fld/Fdr electron donor system in comparison to the reduction with $Na_2S_2O_4$ (solid line). (II) P450 recovery in the reconstituted enzyme reaction after incubation at 37 °C for 20 min in comparison with the original amount (solid line). The dashed line indicates interaction in the presence of substrate, and the dotted line indicates interaction in the absence of substrate.

are caused by low efficiency of electron transfer supported by nonhomologous electron donor systems in vitro. In our reconstituted reaction for human CYP51 the efficiency of enzymatic reduction reaches 95% (data not shown). High turnover number increases the difference between normal activity and the lowest detectable limit; however, no LS conversion was observed upon substitution of the conserved residues corresponding to MTCYP51 Y76 and F83, even though the mutants (Y131F and F139Y) are well expressed and after purification do not show any spectral differences from WT (Supporting Information). Substitution of G141, which in MTCYP51 separates the B′ helix and BC loop (G84), results in a mutant (G141A) having only a trace of the WT activity (64 times decrease in turnover number). The protein must be remarkably destabilized because after 10 min of reaction there was no detectable P450 in the mixture. At a very low level V143A is also expressed as a P450. The activity of the mutant is relatively normal, supporting our assumption that the conservation of the residue (V87 in MTCYP51) is important for protein folding rather than for sterol 14α-demethylation. The results imply that there might be similarity in the organization of SRS1 for water-soluble and membrane-bound isoforms of 14αDM and the motif (YxxxxxpxFGxxV) might be used to suggest CYP51 function of unknown protein sequences.

D146 corresponding to MTCYP51 D90 was the only functionally essential residue in the bacterial isoform for which substitution in the human orthologue does not lead to

Table 4: Mutants of Human CYP51

residue in human CYP51	corresponding residue in MTCYP51	P450 expression, % of WT[a]	14αDM activity[b] LS conversion after 10 min, % (% of WT)	14αDM activity[b] calcd turnover number, min^{-1} (% of WT)
WT		100	81 ± 2 (100)	16.0 ± 1 (100)
Y131F	Y76	55	nd (0)	
F139Y	F83	80	nd (0)	
G140A	G84	28	4 ± 0.5 (5)	0.25 ± 0.05 (1.6)
V143A	V87	8	72 ± 7 (89)	13.5 ± 0.8 (84)
D146A	D90	70	44 ± 7 (54)	4.1 ± 0.05 (26)

[a] P450 expression of WT is 250 ± 50 nmol/L. [b] Parameters were determined as described in Experimental Procedures.

profound effect, although the D146A mutant has a 4-fold decreased turnover number. Differences in the importance of the aspartate may reflect the altered position of the BC loop, probably embedded into the membrane in microsomal P450s (*22*).

CONCLUSIONS

The classical P450 catalytic cycle begins with its interaction with the substrate accompanied by conformational rearrangements which stabilize the enzyme and increase its reduction potential and affinity for protein−protein interaction with electron donor partners (*50*). It has been detected crystallographically that the major changes upon P450 ligand binding occur in the position of secondary structural elements including the three N-terminal SRSs (*53*−*58*). The experimental results of the present study show that 8 of the 10 conserved residues in the B′ helix/BC loop and helices F and G are essential for formation of the productive enzyme/substrate complex in MTCYP51.

Participation of D90 in the interaction with the substrate supports our previous suggestion that closing of the BC loop occurs upon MTCYP51 function (*13*). Exposure to the surface is not typical for P450 heme, and alterations in the BC loop position might be the reason for both the unusually rapid denaturation of the substrate-free form in the reduced CO complexes of this water-soluble isoform and profound stabilization when the fraction of substrate-bound molecules increases. If we assume that surface recognition of the substrate takes place before the loop closing, the 3β-OH of the sterol core is the most plausible group for the interaction with COOH of the aspartate. Closing the BC loop would bring sterol-bound D90 nearer to the heme at the position where it becomes a portion of the ceiling of the active site (Figure 5). Further substrate orientation must include formation of hydrophobic contacts with amino acid residues inside the substrate binding cavity, which would anchor the sterol 14α-methyl group in a spatial position approximately 5 Å from the iron during the three cycles of monooxygenation. In the case of the suggested interaction between the substrate and D90, the sterol side chain would be oriented toward L172 and the hydrophobic arm of R194, while its methyl group at position 10 may make contact with the aromatic ring of F83. Involvement of L172 and R194 in substrate binding and 14α-demethylation requires movement of helices F and G closer to the heme (Figure 5, Table 1). The movement in helices F and G aimed at positioning catalytically important residues at functional sites might occur either simultaneously, with the decrease in the bend of the helix I, as was suggested

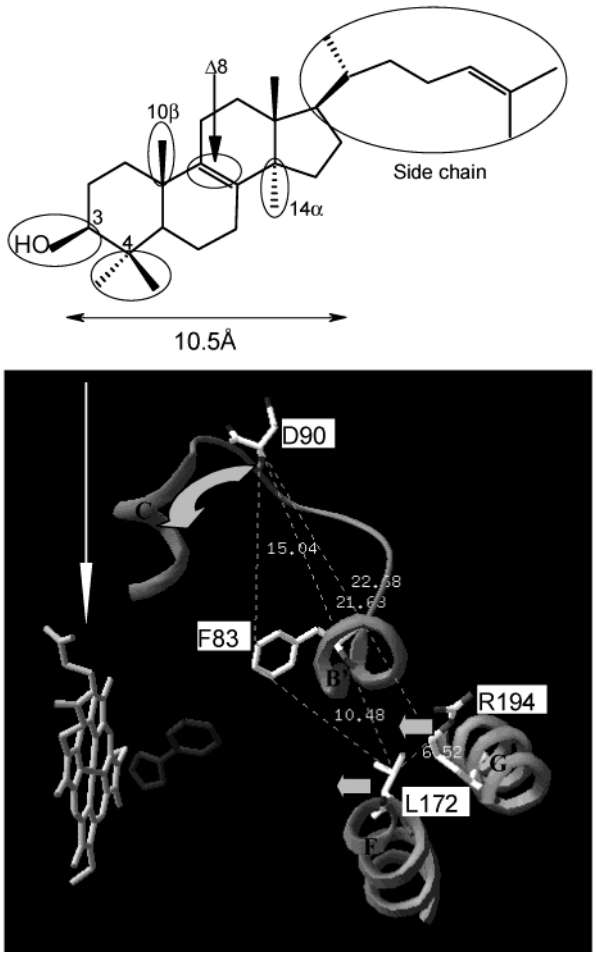

FIGURE 5: Suggested interaction of MTCYP51 with substrate. (Top) Groups in CYP51 substrates essential for 14α-demethylation (ovals). 10.5 Å = the length of the sterol core. The length of the whole molecule varies from 16 to 19 Å as the side chain adopts different conformations (*63*). (Bottom) Location of F83, D90, L172, and R194 in the MTCYP51 structure. Distances between indicated residues in MTCYP51 (Å) are drawn as dashes. The thin arrow shows substrate access channel I (*13*). Thick arrows depict predicted directions of movement of D90, L172, and R194 upon substrate binding.

earlier (*13*) and known to occur in CYP102 (*55*), or independently, resembling the changes found in CYP101 upon interaction with ruthenium-linking substrates where the spatial positions of helices F and G change to adopt the length of the hydrophobic arm of the ligand (*57*).

The essential role of the conserved glycines (G84 and G175) for MTCYP51 activity and formation of the functional enzyme/substrate complex as well as influence of their substitution on the efficiency of enzymatic reduction implies their contribution to the functionally important independent flexibility of the individual secondary structural elements. Replacement of these glycines with alanine, which has high helical propensity, might restrict the local mobility of the polypeptide chain or even prevent proper loop formation, extending the length of helices B′ and F. Increased flexibility of the middle part of helix G or even interruption of the helical structure after mutation A197G may also facilitate conformational rearrangements in the location of the N-terminal part of helix G upon substrate binding and thus lead to greater activity. The results show that the detected 7-fold activation of the mutant is directly connected with an

increased fraction of the substrate-bound molecules of the enzyme. Crystallization of the mutant in the substrate-bound state would give the direct answer, and such studies are underway.

To summarize, we suggest that four of the conserved residues located in the three N-terminal SRSs (F83, D90, L172, and R194) may form direct contacts with substrate, Y76 and D195 maintain proper orientation of heme and R194, respectively, and two glycines control conformational flexibility of the secondary structural elements upon formation of the enzyme/substrate complex. While having quite different roles, the combination of these residues is essential, disruption of any one leading to loss of activity.

These requirements of the enzyme structure correspond well with the strict requirements for the 14αDM substrates (*4*, *8*, *42*). To be 14α-demethylated, a sterol molecule must contain a 3*β*-OH group, at least one methyl group at position 4, a methyl group at position 10*β*, a double bond in the B ring, and a hydrophobic side chain (Figure 5). Absence of any one of these groups prevents metabolism. Probably all of these groups of substrates form weak but multiple, predominantly hydrophobic contacts with the enzyme. Formation of this combination of specific contacts, when substrate becomes an integral part of the enzyme molecule, might be required to achieve the energy state necessary for catalysis (*59*).

The increasing number of available P450 structures strongly supports the observation made after comparison of the first three known P450 folds (*20*); the secondary structural elements which include the three N-terminal SRSs turn out to be not only the most variable in their length but also the most flexible and variable in spatial location in each structure. The CYP superfamily consists of more than 2500 proteins (http://drnelson.utmem.edu), which have only three absolutely conserved amino acid residues, yet acquire essentially the same three-dimensional structure to metabolize more than 10000 organic substrates (*50*, *60*−*62*). It is likely that combination of specific amino acid composition and conformational flexibility of the secondary structural elements defining substrate specificity provides a molecular basis for the multipurpose applicability of the P450 fold.

ACKNOWLEDGMENT

We thank to Dr. J. H. Capdevila for advice on HPLC analysis and D. Mushrush for providing rat P450 reductase.

SUPPORTING INFORMATION AVAILABLE

Substrates of 14αDM, complete sequence alignment of CYP51 family proteins, and HPLC profiles of LS 14α-demethylation by MT and human CYP51, WT, and mutants. This material is available free of charge via the Internet at http://pubs.acs.org.

REFERENCES

1. Yoshida, Y. (1993) Sterol biosynthesis, in *Cytochrome P-450* (Omura, T., Ishimura, Y., and Fujii-Kuriyama, Y., Eds.) 2nd ed., pp 93−101, Kodansha, Tokyo.
2. Yoshida, Y., Aoyama, Y., Noshiro, M., and Gotoh, O. (2000) *Biochem. Biophys. Res. Commun. 273*, 799−804.
3. Trzaskos, J. M., Fischer, R. T., and Favata, M. F. (1986) *J. Biol. Chem. 261*, 16937−16942.
4. Fischer, R. T., Trzaskos, J. M., Magolda, R. L., Ko, S. S., Brosz, C. S., and Larsen, B. (1991) *J. Biol. Chem. 266*, 6124−6132.
5. Shyadehi, A. Z., Lamb, D. C., Kelly, S. L., Kelly, D. E., Schunck, W. H., Wright, J. N., Corina, D., and Akhtar, M. (1996) *J. Biol. Chem. 271*, 12445−12450.
6. Bellamine, A., Mangla, A. T., Nes, W. D., and Waterman, M. R. (1999) *Proc. Natl. Acad. Sci. U.S.A. 96*, 8937−8942.
7. Lamb, D. C., Kelly, D. E., and Kelly, S. L. (1998) *FEBS Lett. 425*, 263−265.
8. Aoyama, Y., Yoshida, Y., Sonoda, Y., and Sato, Y. (1992) *Biochim. Biophys. Acta. 1122*, 251−255.
9. Aoyama, Y., Noshiro, M., Gotoh, O., Imaoka, S., Funae, Y., Kurosawa, N., Horiuchi, T., and Yoshida, Y. (1996) *J. Biochem. (Tokyo) 119*, 926−933.
10. Nelson, D. R. (1999) *Arch. Biochem. Biophys. 369*, 1−10.
11. Marichal, P., Koymans, L., Willemsens, S., Bellens, D., Verhasselt, P., Luyten, W., Borgers, M., Ramaekers, F. C., Odds, F. C., and Bossche, H. V. (1999) *Microbiology 145*, 2701−2713.
12. Asai, K., Tsuchimori, N., Okonogi, K., Perfect, J. R., Gotoh, O., and Yoshida, Y. (1999) *Antimicrob. Agents Chemother. 43*, 1163−1169.
13. Podust, L. M., Poulos, T. L., and Waterman, M. R. (2001) *Proc. Natl. Acad. Sci. U.S.A. 98*, 3068−3073.
14. Jackson, C. J., Lamb, D. C., Marczylo, T. H., Warrilow, A. G., Manning, N. J., Lowe, D. J., Kelly, D. E., and Kelly, S. L. (2002) *J. Biol. Chem. 277*, 46959−46965.
15. Jackson, C. J., Lamb, D. C., Marczylo, T. H., Parker, J. E., Manning, N. L., Kelly, D. E., and Kelly, S. L. (2003) *Biochem. Biophys. Res. Commun. 301*, 558−563.
16. Gotoh, O. (1992) *J. Biol. Chem. 267*, 83−90.
17. Negishi, M., Uno, T., Darden, T. A., Sueyoshi, T., and Pedersen, L. G. (1996) *FASEB J. 7*, 683−689.
18. von Wachenfeld, C., and Jonson, E. F. (1995) in *Cytochrome P450: Structure, Mechanism, and Biochemistry* (Ortiz de Montellano, P. R., Ed.) 2nd ed., pp 183−225, Plenum Publishing Corp., New York.
19. Lewis, D. F. (1998) *Xenobiotica 7*, 617−661.
20. Hasemann, C. A., Kurumbail, R. G., Boddupalli, S. S., Peterson, J. A., and Deisenhofer, J. (1995) *Structure 3*, 41−62.
21. Graham, S. E., and Peterson, J. A. (1999) *Arch. Biochem. Biophys. 369*, 24−29.
22. Williams, P. A., Cosme, J., Sridhar, V., Johnson, E. F., and McRee, D. E. (2000) *Mol. Cell 1*, 121−131.
23. Loughran, P. A., Roman, L. J., Aitken, A. E., Miller, R. T., and Masters, B. S. (2000) *Biochemistry 39*, 15110−15120.
24. Khan, K. K., He, Y. Q., Domanski, T. L., and Halpert, J. R. (2002) *Mol. Pharmacol. 61*, 495−506.
25. Kahn, R. A., Le Bouquin, R., Pinot, F., Benveniste, I., and Durst, F. (2001) *Arch. Biochem. Biophys. 391*, 180−187.
26. Nakayama, K., Puchkaev, A., and Pikuleva, I. A. (2001) *J. Biol. Chem. 276*, 31459−31465.
27. Chen, J. S., Berenbaum, M. R., and Schuler, M. A. (2002) *Insect. Mol. Biol. 2*, 175−186.
28. Koo, L. S., Immoos, C. E., Cohen, M. S., Farmer, P. J., and Ortiz de Montellano, P. R. (2002) *J. Am. Chem. Soc. 124*, 5684−5691.
29. Conley, A., Mapes, S., Corbin, C. J., Greger, D., and Graham, S. (2002) *Mol. Endocrinol. 7*, 1456−1468.
30. Lepesheva, G. I., Podust, L. M., Bellamine, A., and Waterman, M. R. (2001) *J. Biol. Chem. 276*, 28413−28420.
31. Jenkins, C. M., and Waterman, M. R. (1998) *Biochemistry 37*, 6106−6113.
32. Stromstedt, M., Rozman, D., and Waterman, M. R. (1996) *Arch. Biochem. Biophys. 329*, 73−81.
33. Omura, T., and Sato, R (1964) *J. Biol. Chem. 239*, 2379−2385.
34. Nakayama, K., Puchkaev, A., and Pikuleva, I. A. (2001) *J. Biol. Chem. 276*, 31459−31465.
35. Cupp-Vickery, J. R., Garcia, C., Hofacre, A., and McGee-Estrada, K. (2001) *J. Mol. Biol. 311*, 101−110.
36. Kirton, S. B., Baxter, C. A., and Sutcliffe, M. J. (2002) *Adv. Drug Deliv. Rev. 54*, 385−406.
37. Dai, R., Pincus, M. R., and Friedman, F. K. (2000) *Cell. Mol. Life Sci. 57*, 487−499.
38. Nitahara, Y., Aoyama, Y., Horiuchi, T., Noshiro, M., and Yoshida, Y. (1999) *J. Biochem. (Tokyo) 126*, 927−933.
39. Aoyama, Y., Horiuchi, T., Gotoh, O., Noshiro, M., and Yoshida, Y. (1998) *J. Biochem. (Tokyo) 124*, 694−696.
40. Mueller, E. J., Loida, P. J., and Sligar, S. G. (1995) in *Cytochrome P450: Structure, Mechanism, and Biochemistry* (Ortiz de Montellano, P. R., Ed.) 2nd ed., pp 83−124, Plenum Publishing Corp., New York.

41. Brock, B. J., and Waterman, M. R. (1999) *Biochemistry 38*, 1598−1606.
42. Bellamine, A., Mangla, A. T., Dennis, A. L., Nes, W. D., and Waterman, M. R. (2001) *J. Lipid Res. 42*, 128−136.
43. Aoyama, Y., Yoshida, Y., Sonoda, Y., and Sato, Y. (1987) *J. Biol. Chem. 262*, 1239−1243.
44. Mueller, E. J., Loida, P. J., and Sligar, S. G. (1995) in *Cytochrome P450: Structure, Mechanism, and Biochemistry* (Ortiz de Montellano, P. R., Ed.) 2nd ed., pp 83−124, Plenum Publishing Corp., New York.
45. Schlichting, I., Berendzen, J., Chu, K., Stock, A. M., Maves, S. A., Benson, D. E., Sweet, R. M., Ringe, D., Petsko, G. A., and Sligar, S. G. (2000) *Science 287*, 1615−1622.
46. Loffler, J., Kelly, S. L., Hebart, H., Schumacher, U., Lass-Florl, C., and Einsele, H. (1997) *FEMS Microbiol. Lett. 151*, 263−268.
47. Ortiz de Montellano, P. R., and Correia, M. A. (1995) in *Cytochrome P450: Structure, Mechanism, and Biochemistry* (Ortiz de Montellano, P. R., Ed.) 2nd ed., pp 83−124, Plenum Publishing Corp., New York.
48. Mathieu, A. P., LeHoux, J. G., and Auchus, R. J. (2003) *Biochim. Biophys. Acta 1619*, 291−300.
49. Kahn, R. A, Bak, S., Olsen, C. E., Svendsen, I., and Moller, B. L. (1996) *J. Biol. Chem. 271*, 32944−32950.
50. Anzenbacher, P., and Anzenbacherova, E. (2001) *Cell. Mol. Life Sci. 58*, 737−747.
51. Lewis, D. F. V. (1996) *Cytochrome P450: Structure, Function, and Mechanism*, Taylor and Francis, Bristol, PA.
52. Chien, J. Y., Thummel, K. E., and Slattery, J. T. (1997) *Drug Metab. Dispos. 10*, 1165−1175.
53. Ravichandran, K. G., Boddupalli, S. S., Hasermann, C. A., Peterson, J. A., and Deisenhofer, J. (1993) *Science 261*, 731−736.
54. Li, H., and Poulos, T. L. (1996) *Biochimie 78*, 695−699.
55. Li, H., and Poulos, T. L. (1997) *Nat. Struct. Biol. 2*, 140−146.
56. Li, H., and Poulos, T. L. (1999) *Biochim. Biophys. Acta 1441*, 141−149.
57. Dunn, A. R., Dmochowski, I. J., Bilwes, A. M., Gray, H. B., and Crane, B. R (2001) *Proc. Natl. Acad. Sci. U.S.A. 98*, 12420−12425.
58. Park, S., Yamane, K., Adachi, S., Shiro, Y., Weiss, K., Maves, S., and Sligar, S. (2002) *J. Inorg. Biochem. 91*, 491−501.
59. Hammes, G. G. (2002) *Biochemistry 41*, 8221−8228.
60. Werck-Reichhart, D., and Feyereisen, R. (2000) *Genome Biol. 1*, 3003.1−3003.9.
61. Newcomb, M., Hollenberg, P. F., and Coon, M. J. (2003) *Arch. Biochem. Biophys. 409*, 72−79.
62. Danielson, P. B. (2002) *Curr. Drug Metab. 6*, 561−597.
63. Haines, T. H. (2001) *Prog. Lipid Res. 40*, 299−324.

BI034663F